

# Influence of COVID-19 Lockdown on Aerosol Optical Depth over Pokhara and Kyanjin Gompa in Nepal

Ashok Silwal (✉ [ashoksilwal0@gmail.com](mailto:ashoksilwal0@gmail.com))

Patan Multiple Campus, Tribhuvan University, Patandhoka, Lalitpur, Nepal <https://orcid.org/0000-0001-6286-2106>

Sujan Prasad Gautam

Central Department of Physics, Tribhuvan University, Kirtipur, Kathmandu, Nepal

Monika Karki

Amrit Campus, Tribhuvan University, Kathmandu, Nepal

Prakash Poudel

Patan Multiple Campus, Tribhuvan University, Patandhoka, Lalitpur, Nepal

Arati Thapa

Patan Multiple Campus, Tribhuvan University, Patandhoka, Lalitpur, Nepal

Narayan Prasad Chapagain

Amrit Campus, Tribhuvan University, Kathmandu, Nepal

Binod Adhikari

St. Xavier's College, Tribhuvan University, Kathmandu, Nepal

---

## Research Article

**Keywords:** Aerosol, Aerosol Optical Depth, anthropogenic, COVID-19, Correlation

**Posted Date:** June 30th, 2021

**DOI:** <https://doi.org/10.21203/rs.3.rs-669527/v1>

**License:**  This work is licensed under a Creative Commons Attribution 4.0 International License.

[Read Full License](#)

---

# Abstract

The outbreak of the COVID-19 pandemic and the subsequent global economic shutdown provided an opportunity to conduct a real-time experiment assessing the influence of global emission reductions in the Aerosol Optical Depth (AOD) level, an indicator of air pollution over Nepal. Nepal's government imposed a lockdown on the country for approximately three months (from 24 March onwards) in 2020. The purpose of this study is to examine the temporal fluctuation in Aerosol Optical Depth (AOD) caused by the COVID-19 shutdown by comparing its value during the same time period of the past year over two sites: Pokhara and Kyanjin Gompa. We comparatively analyzed the variation of diurnal mean and monthly average AOD of two selected sites, from the month of January to May 2020 and January to May 2018. By examining the time-series graph of daily average AOD prior to and during the lockdown period, our study showed an apparent fluctuation in AOD throughout the studied areas. The major findings of the research revealed that after the lockdown, a significant variation in monthly averaged AOD was observed, ranging from 20–60% deviation over Pokhara and 25–50% deviation in Kyanjin Gompa at different wavelengths. This confirms previous studies on aerosols and other particulate matter during COVID-19 lockdown, as well as theoretical assumptions. In addition, we performed the heatmap correlation analysis among AOD, Total precipitable water (Tpw), Angstrom exponent ( $\alpha$ ), Turbidity coefficient ( $\beta$ ), and Visibility ( $V$ ) during the studied period with possible explanations. We believe this research work serves as a crucial reference for our government to implement appropriate policies for pollution control over the studied areas in the future.

## 1. Introduction

The minute solid particles or liquid droplets suspended in the atmosphere are known as an aerosol. Atmospheric aerosols are mainly produced by the mechanical disintegration processes occurring over land (e.g., lift of dust) and ocean (e.g., sea-spray) and by chemical reactions occurring in the atmosphere [1, 2]. Natural aerosols such as dust, fly ash, soot, pollen grains, and carbon particle occur naturally as they mix in the atmosphere by different natural phenomena, thereby covering the majority of the aerosol in the atmosphere, on the other hand, anthropogenic aerosols are located considerably in a polluted area due to human activities, including fossil fuel combustion, biomass burning, industrial smoke, power plants, coal mining, and other several activities, overlaying approximately 10% of the entire aerosols [3]. These different aerosol groups often clump together to form a hybrid of both natural and anthropogenic. Aerosols can make their way into the atmosphere almost everywhere globally, depending on the season and weather conditions [2].

Aerosol scatters and absorb sunlight (size range 0.1-1 micrometres are most effective) [4, 5] and change the cloud's characteristics [6]. They directly affect limiting visibility and causing a risk to human health, including premature deaths, allergies, respiratory problems such as Influenza, Pneumonia, and harmful cardiovascular effects such as heart attacks and strokes [3, 7, 8]. On examining the long-term records of aerosol particles and lung cancer incidence, Tie et al. [9] reported that the mortality due to lung cancer is

aerosol pollution causes wide-ranging consequences for human health, natural ecosystems, visibility, weather, radiative forcing, and tropospheric oxidation (self-cleaning) capacity [10]. In addition, aerosols influence the melting of snow and ice in the Himalayas and around the Tibetan Plateau, which ultimately plays a crucial role in climate change [11].

Aerosol Optical Depth (AOD) is an optical measure of light extinction (absorption and scattering) of the solar beam due to the number of total aerosols in the entire atmospheric column and provides an indirect measure of aerosols in the atmosphere [3]. As aerosol deposition is continually rising due to industrialization and urbanization, high population density, or biomass burning in different regions of Nepal, aerosols studies, particularly AOD, has risen rapidly in recent years [12]. In the past, several works (e.g., Acharya et al. [3], Bhattarai et al. [6] Jha et al. [7], Regmi et al. [11], Regmi et al. [12], Chapagain [13], Carrico et al. [14]) were executed in Kathmandu, Pokhara and other different sites over Nepal to measure and study of particulate matter such as total suspended particulate matter (TSP), polycyclic aromatic hydrocarbons (PAH), Black Carbon (BC), AOD and some gaseous pollutants.

The COVID-19 pandemic has impacted each thing of human lifestyles and the worldwide economy. Depending on the extent of its impact, the authorities of different nations were adopting distinctive ranges of involvement, such as tour restrictions, shutting down factories, industrial activities, and other social activities to manipulate the unfold of the relatively contagious virus. Several studies, such as Sharma et al. [15], Tobias et al. [16], Abdullah et al. [17], Acharya et al. [18], Chauhan and Singh [19], Bao & Zhang [20], over the different regions of the globe; India, Spain, Malaysia, Europe, USA, China, has claimed that lockdown had contributed significantly in improving air quality due to decrement in emission. Ranjan et al. [21] aimed to study the effect of the Covid-19 pandemic on aerosol optical depth, concluding a huge reduction in AOD, about 6% to 45 %, over the different regions of India. Acharya et al. [18] revealed that lockdown reduced AOD by ~ 20% at maximum places in Europe and USA. Raza et al. [22] reported that AOD was reduced in Pakistan during the lockdown period in 2020 in comparison to the previous years. From the worldwide study of AOD during the pandemic period, Sanap [23] recorded a decrease in AOD from mid-March to April 2020; however, a drastic reduction in AOD was observed in May. Furthermore, despite many impacts of lockdown on people's social life and the national economy, several findings [e.g., Shrestha et al. [24], Gautam et al. [25], Baral & Thapa [26] observed that lockdown had temporarily better environmental conditions in Nepal.

In this particular paper, we present results on the implications of observed diurnal and monthly averaged variation of aerosol optical depth due to anthropogenic aerosols over the two sites of Nepal by dividing the study into two scenarios, i.e., before the lockdown (1 January 2020–23 March 2020) and during the lockdown (24 March 2020–31 May 2020). We emphasized the variation of anthropogenic aerosol pollution in the most polluted and the least polluted regions. This work is also based on the observational findings utilizing Total Precipitable Water (Tpw) and visibility correlation with their respective AOD wavelength during the study period. This paper is organized as follows: in Sect. 2, we describe the methodology, in Sect. 3, we discuss the results, and finally, we conclude our study in Sect. 4.

## 2. Materials And Method

### 2.1 Dataset

The required data for this research work has been taken from AERONET provided by GSFC NASA (<https://aeronet.gsfc.nasa.gov/>). The Aerosol Robotic Network (AERONET), a ground-based remote sensing aerosol network of well-calibrated Sun/sky radiometers established in the early 1990s, is a well-established and productive facility for passive aerosol measurement [27]. The study site was chosen based on available data for Nepal in order to maximize the use of available databases. Daily averages of all AOD data points were calculated and then examined on a monthly average basis.

### 2.2 Site Selection

Figure 1 shows a network of the stations in the map of Nepal used in this study for AOD observation. More detailed information about the aeronet sites is shown in table 1.

**Table 1:** Locations of the selected site with their geographic latitude and longitude.

Site	Latitude	Longitude	Start date	End date
Pokhara	28.187 <sup>0</sup> N	83.975 <sup>0</sup> E	01 Jan (2018 & 2020)	31 May (2018 & 2020)
Kyanjin_Gompa	28.211 <sup>0</sup> N	85.566 <sup>0</sup> E		

### 2.3 Instrumentation

The CIMEL Electronic CE-318 sun/sky radiometer, which is part of the AERONET worldwide network, was used for all of the observations reported in this paper. This sensor operates by measuring the intensity of solar radiation at any specified wavelength and converting it to optical depth using the corresponding concentrations at the top of the atmosphere [27]. More information about the AERONET equipment utilized for optical depth retrieval can be found in Schmid's work [28]. The AERONET archive is classified into three quality levels: raw data at level 1.0, cloud-screened data at level 1.5, and quality-assured data at level 2.0. The AERONET data used in this work are version 3.0 at level 1.5, which includes cloud exclusion and quality controls, but may lack final calibration.

In this study, AODs of corresponding wavelengths 1640 nm, 1020 nm, 870 nm, 675 nm and 440 nm have been used to analyze diurnal and monthly time series analysis. The spectral AOD () data obtained from the AERONET using the wavelength of 440 – 870 nm is used to calculate the different optical properties of the aerosols as wavelength exponent ( $\alpha$ ), turbidity coefficient ( $\beta$ ), visibility (V) using Angstrom's turbidity law, given by Iqbal et al. [29]:

$\beta$  represents the amount of aerosol presents in the air in the vertical column of the atmosphere, while  $\alpha$  is related to the size distribution of aerosol in the atmosphere, having the value ranging from 0 to 4. We calculate  $\alpha$  from the wavelength of 440 – 870 nm by using the formula provided by Sayer et al. [30]:

**See formula 2 in the supplementary files.**

where  $r_1$  and  $r_2$  are the AOD at wavelengths  $\lambda_1$  and  $\lambda_2$ .

The higher value of  $\alpha$  indicates the higher percentage of smaller sized aerosol particles in the air and vice versa [31, 32].

Additionally, visibility was investigated, which is defined as the degree of clarity or the farthest distance through the atmosphere to the horizon at which prominent objects may be distinguished with the naked eye. Its value in km can be computed by using the following formula [29].

**See formula 3 in the supplementary files.**

## 3. Result And Discussion

Based on the methodology and datasets discussed above, AOD data were analyzed on two sites: Kyanjin Gompa and Pokhara, from January to May for the years 2020 and 2018. The data within (1 January – 23 March) represents the days before lockdown, while the other days (24 March – 31 May) represent the lockdown period. The choice of this time was made to investigate the AOD variations due to the decrease in the anthropogenic aerosols during the lockdown period. Based on anthropogenic activities, the two sites, Pokhara and Kyanjin Gompa, were considered the most polluted region and the least polluted region.

### 3.1 Diurnal Variation of mean AOD

The variation of mean diurnal AOD at 440 nm, 675 nm, 870 nm, 1020 nm, and 1640 nm for the period of January to May in 2020 and 2018 over the sites, Kyanjin Gompa and Pokhara, are shown in Figs. 2 and 3, respectively.

The above figures illustrate that both studied sites had the most aerosol loading at wavelength 440 nm with the variant of time followed by other wavelengths in increasing order. This means that the submicron aerosol particle is dominant in this vicinity than that of coarse mode aerosol. The dominance of shorter wavelength AOD was also reported in different literatures [7, 33, 34]. Minimum aerosols loading in the atmosphere was observed during the month of January, which may be due to the weak generation mechanisms as well as the colder ground surface. The higher AOD over Pokhara (above 0.3 for most cases) signifies that Pokhara and the surrounding around the valley are heavily polluted [35, 36]. On the other hand, the AOD was recorded below 0.4 for all studied periods over the site Kyanjin\_Gompa.

In addition, the daily mean AOD varied significantly with months along with the AERONET sites Pokhara and Kyanjin\_Gompa. During the end days of February 2020, the AOD at different wavelengths exhibited dispersion with a significantly high value in comparison to the same time frame of 2018. However, AOD varied within a low range in March of 2020 in comparison to 2018. The time-series analysis also revealed that the AOD maintained by particles of different wavelengths were below 2.0 during the lockdown period, as observed from the AERONET site Pokhara. This value was recorded below 0.25 in Kyanjin\_Gompa. During the same months of 2018, the aerosol particle of wavelength 440 attained the peak value of 3.40 in April and 0.35 in May over Pokhara and Kyanjin\_Gompa. Similarly, particles with other wavelengths also showed variation with a large value during April - June of 2018 compared to the same period of 2020. These results reflect the positive impact of lockdown on air quality. It might be due to the cut down of predominant aerosol sources like traffic and factory operation. A significant reduction in AOD anomaly due to lockdown was also observed across the different regions of the globe [18, 21, 23].

## 3.2 Monthly variation of mean AOD

Figures 4 and 5 represent the monthly variations of the average AOD and percentage deviation in AOD of the Kyanjin\_Gompa, and Pokhara, respectively. The monthly average AOD of the Pokhara and Kyanjin\_Gompa were the least for January at 1640 nm, and the highest values were observed for the month of February and April, respectively, at 675 nm. The maximum recorded monthly average AOD was 0.53 (in 2020) & 0.60 (in 2018) for Pokhara; on the other hand, the highest AOD of 0.07 (in 2020) & 0.09 (in 2018) was obtained for Kyanjin\_Gompa. Quite less value of AOD in Kyanjin\_Gompa than in Pokhara can be noticed due to its location, Kyanjin\_Gompa lies in the Himalayan region (a very less polluted region in Nepal), but Pokhara is an urban area that has the possibility of maximum pollutants emission. The comparative analysis of these two sites, with the same period of 2018, depicts that AOD was decreased drastically in the month of March, April, and May in both stations, which clearly shows the effects due to lockdown. Overall, the monthly deviation of AOD (at different wavelengths) during the lockdown period ranges between ~ 25–50% for Kyanjin\_Gompa and ~ 20–60% for Pokhara, with a maximum decrement of AOD in the month of March. This result is consistent with the global study of AOD during the lockdown period by Sanap [23]. However, comparatively less deviation in AOD was observed in the month of April and May. The decrement in AOD in our study regions during lockdown is more than in the different areas of India (6 to 45% as recorded by Ranjan et al. [21]) and Europe (~ 20% observed by Acharya et al. [18]). During the lockdown, the production of the anthropogenic aerosol has decreased, which resulted in the lowering of the monthly average AOD, thus enhancing the fact that human activities that help in the production of anthropogenic aerosols are significant factors affecting AOD.

## 3.3 Correlation Analysis: Heat map

Different forms of correlation analysis, such as Pearson's correlation, Cross-correlation analysis, correlation using Heatmap, have been widely used as a powerful tool to establish the relationship between two time-series data. Various studies (e.g., Silwal et al. [37, 38], Thapa et al. [39], Poudel et al.

weather and climate change for studying the association between two parameters, revealing physics behind them, and forecasting its impact on the local and global scale.

In this study, we examined the relationship among aerosol parameters. Results in Fig. 6 represent correlation analysis for AOD at wavelengths 870 nm, 440 nm, Total Precipitable Water (Tpw), Angstrom Exponent ( $\alpha$ ), Turbidity Coefficient ( $\beta$ ) through heat map. Here, we compared the correlation analysis of different parameters during January-May of 2020, prior and after lockdown with January-May of 2018 to investigate the effect of lockdown on their correlation coefficient value at Aeronet sites viz.

Kyanjin\_Gompa and Pokhara. Each square shows the correlation coefficients between the different variables on each axis. The correlation coefficient is scaled from +1 to -1, and the value close to 0 indicates there is less or no linear trend between the two variables. The value closer to  $\pm 1$  indicates the strong correlation between them. The figure shows that the principal diagonal coefficients are all 1 (dark red) because those squares correlate each variable to itself, so it is a perfect correlation. A consistent reduction in correlation coefficient was observed among the observational data from 25 March to 31 May (2020) compared to the similar period of 2018. The AOD (870 nm) had a perfect positive correlation of 1 with Turbidity coefficient beta ( $\beta$ ). This is because  $\beta$  refers to the number of aerosols present vertically in the atmosphere. It is noteworthy to mention that AOD (870 nm) was strongly correlated with AOD (440 nm), ranging >0.9 prior to and during the lockdown. The Angstrom Exponent ( $\alpha$ ) had a negative correlation with visibility (V) as indicated by the coefficient of -0.33 before lockdown and -0.015 during the lockdown in 2020, while that of 2018 had a coefficient of -0.21 during 1 January – 24 March and +0.27 during 25 March – 31 May at Kyanjin\_Gompa. The shift in the trend of  $\alpha$  and V from 25 March to 31 May (negative correlation in 2018) to the similar period of 2020 (positive correlation in 2020) is a notable finding. The Tpw had a positive correlation of 0.46 with AOD (440 nm) prior to and 0.23 during 25 March – 31 May, while that of 2018 had 0.68 during 1 January – 24 March and 0.19 during 25 March – 31 May. Similarly, Fig. 6 manifests that the AOD had a negative correlation of -0.62 for the period 1 January – 24 March (2020) and -0.58 with visibility during the lockdown period, while a negative correlation of -0.73 and -0.66 on 25 March – 31 May with respect to that of the year 2018 at Pokhara station. By analyzing the cross-correlation between Tpw and AOD, it can be seen that as the AOD increases, the reflectance spectrum is broadened, and the clouds that generate rainfall increase, resulting in the positive correlation between the precipitation intensity and AOD. Thus, the present study results are in good agreement with the aforementioned studies of Fan et al. [42] and Lebo et al. [43]. The sudden change in correlation coefficient in the period of 25 March – 31 May 2020, compared to the same time period in the year 2018, could be attributed to the influence of COVID-19 lockdown as it caused the shutting down of factories and kept vehicles off the road.

It is worth mentioning that the sensitivity of the Pearson coefficients depends upon the chosen time frame. Correlations can be highly sensitive to the time frame of observation [44]. In particular, when short time frames with few data are analyzed, the correlation parameters may be misleading. Therefore, researchers should carefully scrutinize different correlation regimes before drawing any general conclusions. Principally, the more data analyzed and the longer the time frame, the more meaningful the

correlation results. Therefore, our interest is to compare the long-term mean AOD level of the same periods in the near future.

## 4. Conclusion

This study aims to investigate the aerosol records, AOD variability, from two stations, including one less and one high polluted region of Nepal prior to and after the lockdown period. From the diurnal & monthly variation, and heatmap correlation analysis, we have concluded the following results.

- Studies had shown that the time series of AOD for urban city Pokhara had a comparatively large value than the less polluted site Kyanjin\_Gompa. By investigating the diurnal mean AOD of Pokhara and Kyanjin\_Gompa, it was observed that the maximum AOD values at different wavelengths were recorded up to 1.55 at Pokhara and 0.13 at Kyanjin\_Gompa before lockdown. However, there was a significant decrement in AOD values during the lockdown, which is visible from the comparison of AOD with the same period of the past year.
- During the studied period over Pokhara and Kyanjin\_Gompa, monthly variation in Aerosol Optical Depth showed a drastic fall in AOD compared to the past year. Decrement in AOD was recorded up to 20–60% for Pokhara and 25–50% for Kyanjin\_Gompa. The maximum reduction occurred in March, and a slightly less drop in AOD was observed in other months.
- Restrictions in emissions of various anthropogenic aerosols due to the shutdown of the novel coronavirus pandemic could be the possible reason behind this improvement on aerosols. Other various studies of AOD also supported our results during Covid-19 lockdown at different parts of the globe.
- Correlation analysis among AOD, water precipitation (Tpw), angstrom exponent ( $\alpha$ ), turbidity coefficient ( $\beta$ ), and visibility was performed during the study period. We found quite less value of correlation coefficient for short term analysis; as climate data follows a periodic cycle in the long term and due to the effect of seasonal variation, a higher value of correlation coefficient can be expected for long-term aerosols study. However, our study shows a greater association of AOD with visibility and water precipitation at the least polluted Kyanjin\_Gompa site than at Pokhara.

Considering the threat to the environment and health of the population, the control technologies on the production and emission of a large number of aerosols must be adopted in the polluted regions. We believe that the study of such a measure of aerosols helps well enough to build a solid understanding and a correct illustration of the essential aerosol-cloud-precipitation methods that drive precipitation and the Earth's radiative balance. This could successfully incorporate the understanding of aerosols into regional and global climate models.

## Declarations

**Acknowledgements:** We would like to thank the AERONET database for providing AOD data for this

Loading [MathJax]/jax/output/CommonHTML/jax.js

**Supplementary Materials:** The supplement data can be downloaded from <https://aeronet.gsfc.nasa.gov/>

**Authors' Contributions:** This work was carried out in collaboration with all authors under the guidance of authors N. P. Chapagain and B. Adhikari. There is an equal group effort of all the authors at all stages.

**Conflict of Interest:** The authors declare that they have no conflict of interest.

**Funding:** No funding was sought or obtained to conduct this study.

**Ethical approval:** Not applicable.

## References

1. S. K. Satheesh, Aerosols and climate, *Resonance* 7(4) (2002) 48–59.  
<https://doi.org/10.1007/BF02836138>
2. A. Voiland, Aerosols: Tiny Particles, Big Impact: Feature Articles, 2 November, 2010.  
<https://earthobservatory.nasa.gov/features/Aerosol>
3. A. Acharya, B. Adhikari, P. Bhattarai, G. Jha, S. Acharya, R. Shah, Spectral analysis of aerosol optical depth over AERONET sites of Nepal, *BIBECHANA* 17 (2020) 80–88.  
<https://doi.org/10.3126/bibechana.v17i0.26507>
4. N. Mahowald, S. Albani, J. F. Kok, S. Engelstaeder, R. Scanza, D. S. Ward, Flanner MG. The size distribution of desert dust aerosols and its impact on the Earth system, *Journal of Aeolian Research* 15 (2014) 53–71. <https://doi.org/10.1016/j.aeolia.2013.09.002>
5. P. Chen, S. Kang, C. Li, M. Rupakheti, F. Yan, et al., Characteristics and sources of polycyclic aromatic hydrocarbons in atmospheric aerosols in the Kathmandu Valley, Nepal, *Science of the Total Environment* 538 (2015) 86–92. <https://doi.org/10.1016/j.scitotenv.2015.08.006>
6. B. C. Bhattarai, J. F. Burkhardt, F. Stordal, and C-Y Xu, Aerosol Optical Depth Over the Nepalese Cryosphere Derived from an Empirical Model, *Front. Earth Sci.* 7 (2019) 178.  
<https://doi.org/10.3389/feart.2019.00178>
7. R. Jha, B. Adhikari, D. K. Singh, Study of aerosol optical properties at different tourist places of Nepal, *BIBECHANA* 18 (1) (2021) 170–183. <https://doi.org/10.3126/bibechana.v18i1.29906>
8. M. Iqbal, An Introduction to Solar Radiation, Academic Press, Canada, pp 107–154. ISBN: 0-12-373752-4 (pbk), 1983.
9. X. Tie, D. Wu & G. Brasseur, Lung cancer mortality and exposure to atmospheric aerosol particles in Guangzhou, China, *Atmospheric Environment* 43 (2009) 2375–2377.  
<https://doi.org/10.1016/j.atmosenv.2009.01.036>
10. X. Tie, S. Madronich, S. Walters, D. P. Edwards, P. Ginoux, et al., Assessment of the global impact of aerosols on tropospheric oxidants, *Journal of Geophysical Research: Atmospheres* 110 (D3) (2005).  
<https://doi.org/10.1029/2004JD005359>

11. J. Regmi, K. N. Poudyal, A. Pokhrel, M. Gyawali, et al., Investigation of Aerosol Climatology and Long-Range Transport of Aerosols over Pokhara, Nepal, *Atmosphere* 11 (2020) 874.  
<https://doi.org/10.3390/atmos11080874>
12. J. Regmi, K. N. Poudyal, A. Pokhrel, M. Gyawali, A. Barinelli, R. Aryal, Analysis of Aerosol Optical Depth and Angstrom Exponents over an AERONET site at Pokhara, Nepal, *BIBECHANA* 18 (1) (2021) 118–127. <https://doi.org/10.3126/bibechana.v18i1.29448>
13. N. P. Chapagain, Diurnal Variations of Total Ozone Over Kathmandu Measured by Brewer Spectrophotometer, *The Himalayan Physics* 6 & 7 (2017) 24–30.  
<https://doi.org/10.3126/hj.v6i0.18353>
14. C. M. Carrico, M. H. Bergin, A. B. Shrestha, J. E. Dlb, et al., The importance of carbon and mineral dust to seasonal aerosol properties in the Nepal Himalaya, *Atmospheric Environment* 37 (2003) 2811–2824. [https://doi.org/10.1016/S1352-2310\(03\)00197-3](https://doi.org/10.1016/S1352-2310(03)00197-3)
15. S. Sharma, M. Zhang, Anshika, J. Gao, H. Zhang, S. H. Kota, Effect of restricted emissions 855 during COVID-19 on air quality in India, *Sci. Total Environ.* 728 (2020) 138878.  
<https://doi.org/10.1016/j.scitotenv.2020.138878>
16. A. Tobías, C. Carnerero, C. Reche, J. Massagué, M. Via, et al., Changes in air quality during the lockdown in Barcelona (Spain) one month into the SARS-CoV-2 epidemic, *Sci. Total Environ.* 726 (2020) 138540. <https://doi.org/10.1016/j.scitotenv.2020.138540>
17. S. Abdullah, A. A. Mansor, N. N. L. M. Napi, W. N. W. Mansor, A. N. Ahmed, et al., Air quality status during 2020 Malaysia Movement Control Order (MCO) 701 due to 2019 novel coronavirus (2019-nCoV) pandemic, *Sci. Total Environ.* 702 (2020) 139022.  
<https://doi.org/10.1016/J.SCITOTENV.2020.139022>
18. P. Acharya, G. Barik, B. K. Gayen, S. Bar, et al., Revisiting the levels of Aerosol Optical Depth in South-Southeast Asia, Europe and USA amid the COVID-19 pandemic using satellite observations, *Environmental Research* 193 (2021) 110514. <https://doi.org/10.1016/j.envres.2020.110514>
19. A. Chauhan, and R. P. Singh, Decline in PM2.5 concentrations over major cities around the world associated with COVID-19, *Environ. Res.* 187 (2020) 109634.  
<https://doi.org/10.1016/j.envres.2020.109634>
20. R. Bao, and A. Zhang, Does lockdown reduce air pollution?: Evidence from 44 cities in northern China, *Sci. Total Environ.* 731 (2020) 139052. <https://doi.org/10.1016/J.SCITOTENV.2020.139052>
21. A. K. Ranjan, A. K. Patra, A. K Gorai, Effect of lockdown due to SARS COVID-19 on aerosol optical depth (AOD) over urban and mining regions in India, *Science of the Total Environment* 745 (2020) 141024. <https://doi.org/10.1016/j.scitotenv.2020.141024>
22. D. Raza, M. Ehsan, S. U. Khan, A. Raza, et al., Dire Situation of Covid-19 in Pakistan and its Impact on Aerosol Optical Depth – A Case Study, *BUJES* 5(1) (2020) 7pp.
23. S. D. Sanap, Global and regional variations in aerosol loading during COVID-19 imposed lockdown, *Atmospheric Environment* 246 (2021) 118132. <https://doi.org/10.1016/j.atmosenv.2020.118132>

24. A. Shrestha, R. Sharma, S. Bhattarai, H. Tran, M. Rupakheti, Lockdown caused by COVID-19 pandemic reduces air pollution in cities worldwide, arXiv, Apr. 2020.  
<https://doi.org/10.31223/osf.io/edt4j>
25. S. P. Gautam, A. Silwal, P. Poudel, A. Thapa, P. Sharma, M. Lamsal, M. and R. Neupane, Comparative Study of Ambient Air Quality Using Air Quality Index in Kathmandu City, Nepal, IOSR Journal of Environmental Science Toxicology and Food Technology 14(5) (2020) 29–35.  
<https://www.researchgate.net/publication/343554836>
26. B. D. Baral, and K. Thapa, K., Effect of the COVID-19 Lockdown on Ambient Air Quality in Major Cities of Nepal, Journal of Health and Pollution, 11(29) (2021) 210211. <https://doi.org/10.5696/2156-9614-11.29.210211>
27. B. N. Holben, T. F. Eck, I. Slutsker, D. Tanre, J. P. Buis, et al., AERONET-A federated instrument network and data archive for aerosol characterization, Remote Sens. Environ. (1998) 1–16.  
[https://doi.org/10.1016/S00344257\(98\)00031-5](https://doi.org/10.1016/S00344257(98)00031-5)
28. J. Schmid, J. J. Michalsky, D. W. Slater, J. C. Bernard, R. N. Halthore, J. C. Liljegren, et al., Comparison of columnar water-vapour measurements from solar transmittance methods, Appl. Opt. (2001) 1886–1896. <https://doi.org/10.1364/AO.4000188613>
29. M. Iqbal, An introduction to solar radiation, Elsevier, 2 December, (2012).
30. A. M. Sayer, N. C. Hsu, C. Bettenhausen, & M. J. Jeong, Validation and uncertainty estimate for MODIS Collection 6 "Deep Blue" aerosol data, Journal of Geophysical Research: Atmospheres 118(14) (2013) 7864–7872. <https://doi.org/10.1002/jgrd.50600>
31. A. Ångström, Techniques of determinig the turbidity of the atmosphere. Tellus 13(2) (1961) 214–223.  
<https://doi.org/10.3402/tellusa.v13i2.9493>
32. H. Moosmüller, R. K. Chakrabarty, K. M. Ehlers, & W. P. Arnott, Absorption Ångström coefficient, brown carbon, and aerosols: basic concepts, bulk matter, and spherical particles, Atmospheric Chemistry and Physics 11(3) (2011) 1217–1225. <https://doi.org/10.5194/acp-11-1217-2011>
33. N. Sharma, Variations of Aerosol Optical Depth in Bhaktapur, Nepal, Journal of the Institute of Engineering 13(1) (2018) 133–138. <https://doi.org/10.3126/jie.v13i1.20358>
34. D. R. Reidmiller, P. V. Hobbs, and R. Kahn, Aerosol optical properties and particle size distributions on the east coast of the United States derived from airborne in situ and remote sensing measurements, Journal of the atmospheric sciences 63(3) (2006) 785–814. <https://doi.org/10.1175/JAS3674.1>
35. V. Ramanathan, F. Li, M. V. Ramana, P. S. Praveen, D. Kim, C. E. Corrigan, et al., Atmospheric brown clouds: Hemispherical and regional variations in long-range transport, absorption, and radiative forcing, Journal of Geophysical Research: Atmospheres 112(D22) (2007).  
<https://doi.org/10.1029/2006JD008124>
36. S. Ramachandran, & M. Rupakheti, Inter-annual and seasonal variations in optical and physical characteristics of columnar aerosols over the Pokhara Valley in the Himalayan foothills, Atmospheric Research 248 (2021) 105254. <https://doi.org/10.1016/j.atmosres.2020.105254>

37. A. Silwal, S. P. Gautam, P. Poudel, M. Karki, B. Adhikari, N. P. Chapagain, et al., Global positioning system observations of ionospheric total electron content variations during the 15 January 2010 and 21 June 2020 solar eclipse, *Radio Science* 56(5) (2021) 1–20.  
<https://doi.org/10.1029/2020RS007215>
38. A. Silwal, S. P. Gautam, N. P. Chapagain, M. Karki, P. Poudel, et al., Ionospheric Response over Nepal during the 26 December 2019 Solar Eclipse, *Journal of Nepal Physical Society* 7(1) (2021) 25–30.  
<https://doi.org/10.3126/jnphyssoc.v7i1.36970>
39. A. Thapa, A. Silwal, S. P. Gautam, C. K. Nepal, S. Bhattarai and D. Timsina, Surface air temperature trends in Kathmandu Valley for 2011–2017, *BIBECHANA* 18(2) (2021) 95–104.  
<https://doi.org/10.3126/bibechna.v18i2.29495>
40. P. Poudel, N. Parajuli, A. Gautam, D. Sapkota, H. Adhikari, et al., Wavelet and Cross-Correlation Analysis of Relativistic Electron Flux with Sunspot Number, Solar Flux, and Solar Wind Parameters, *Journal of Nepal Physical Society* 6(2) (2020) 104–112.  
<https://doi.org/10.3126/jnphyssoc.v6i2.34865>
41. M. Karki, A. Silwal, N. P. Chapagain, P. Poudel, S. P. Gautam, et al., GPS Observations of Ionospheric TEC Variations during 2015 Mw 7.8 Nepal Earthquake, *Earth and Space Science Open Archive ESSOAr* (2020). <https://doi.org/10.1002/essoar.10504866.1>
42. J. Fan, D. Rosenfeld, Y. Zhang, S. E. Giangrande, Z. Li, L. A. Machado, et al., Substantial convection and precipitation enhancements by ultrafine aerosol particles, *Science* 359(6374) (2018) 411–418.  
<https://doi.org/10.1126/science.aan8461>
43. Z. J. Lebo, and G. Feingold, G., On the relationship between responses in cloud water and precipitation to changes in aerosol, *Atmospheric Chemistry and Physics* 14(21) (2014) 11817–11831. <https://doi.org/10.5194/acp-14-11817-2014>
44. G. Meissner, The Pearson Correlation Model - Work of the Devil, Retrieved, 4(15) (2015) 2018.

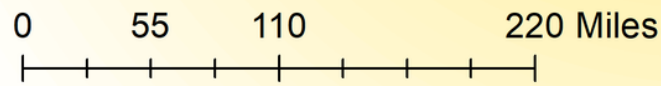
## Figures

# Study Area Map



## Legend

- Aeronet Site (Red flag icon)
- Districts (Green area)



Coordinate System: GCS WGS 1984  
Datum: WGS 1984  
Units: Degree

**Figure 1**

Map showing the aeronet sites from which data was obtained (Source: Created by the author using ArcGIS 10.7 software).

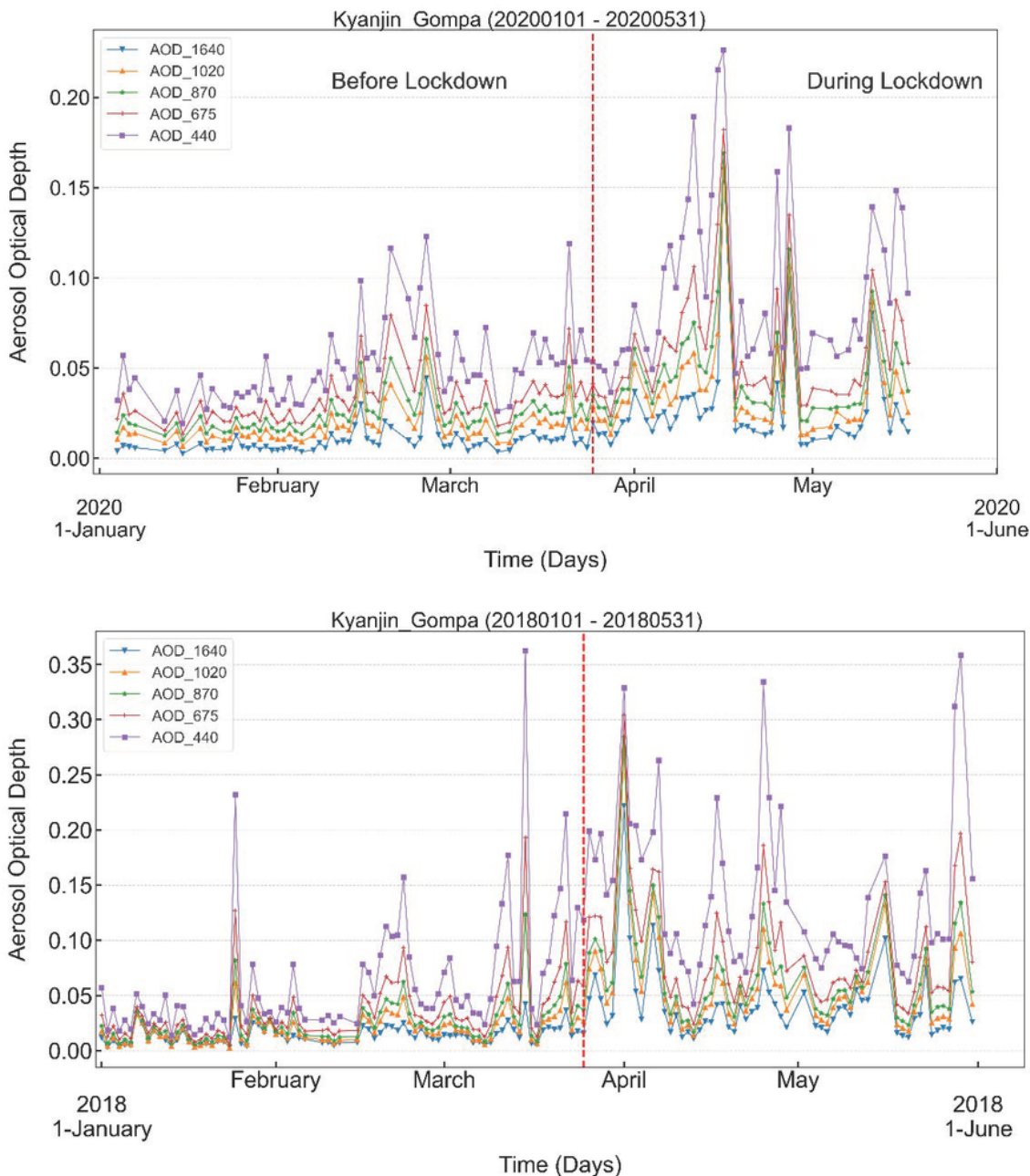


**Figure 2**

AOD time series of Kyanjin Gompa during the period Jan-May, 2020 (upper), and Jan-May 2018 (lower).

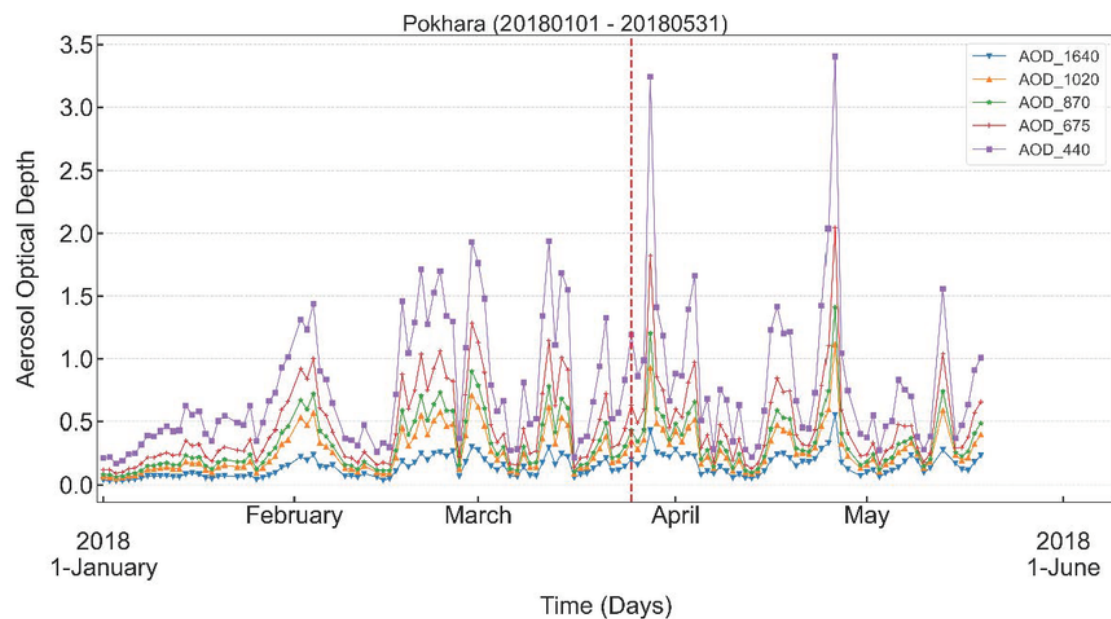
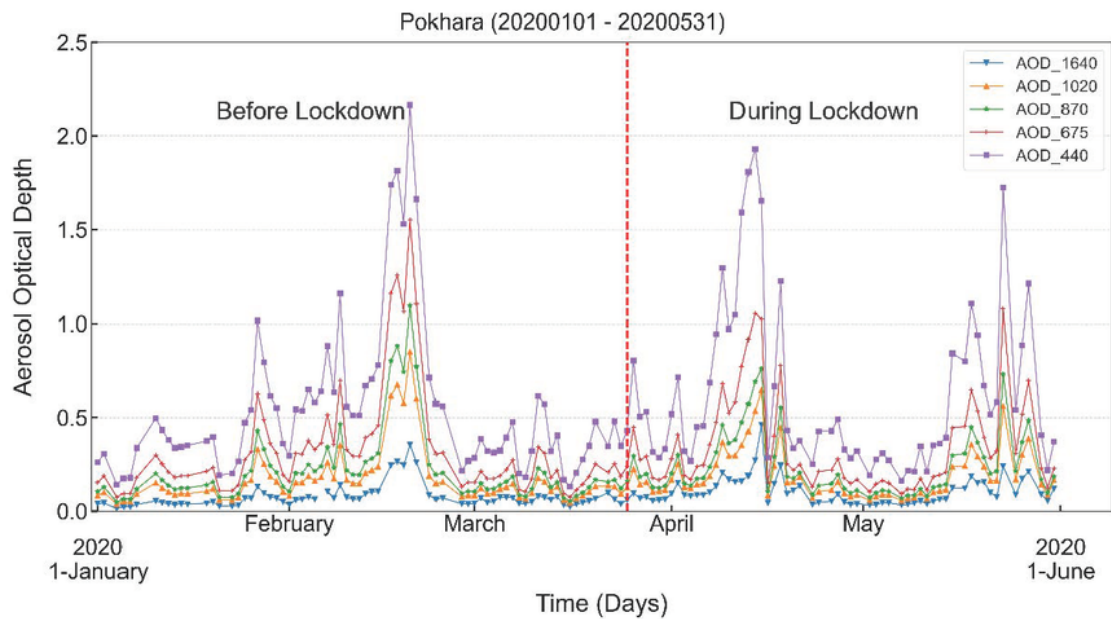


**Figure 3**

AOD time series of Pokhara during the period Jan-May, 2020 (upper) and Jan-May 2018 (lower).

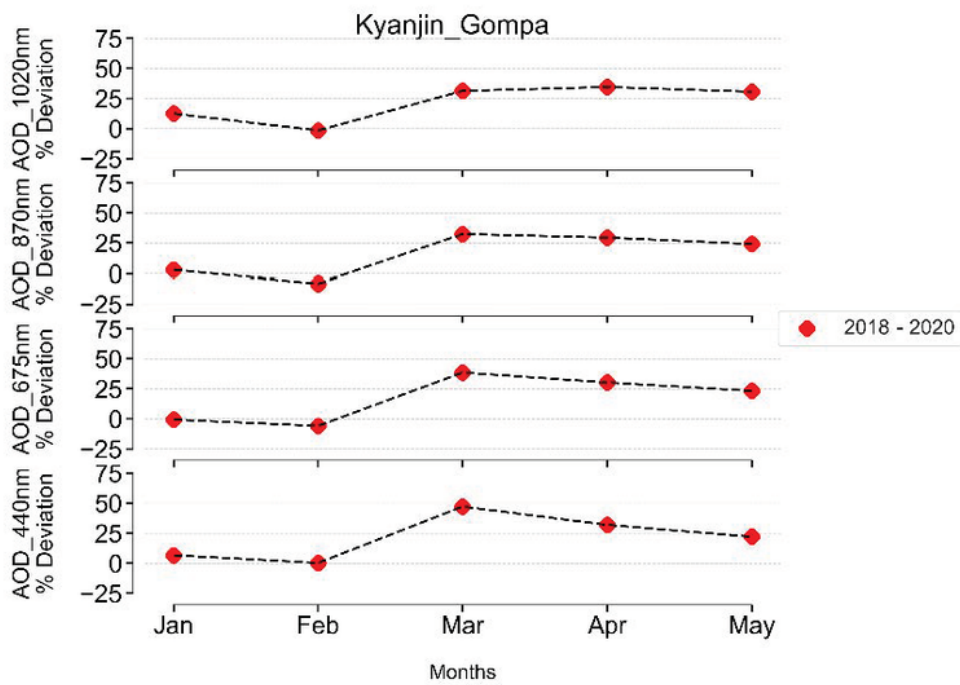
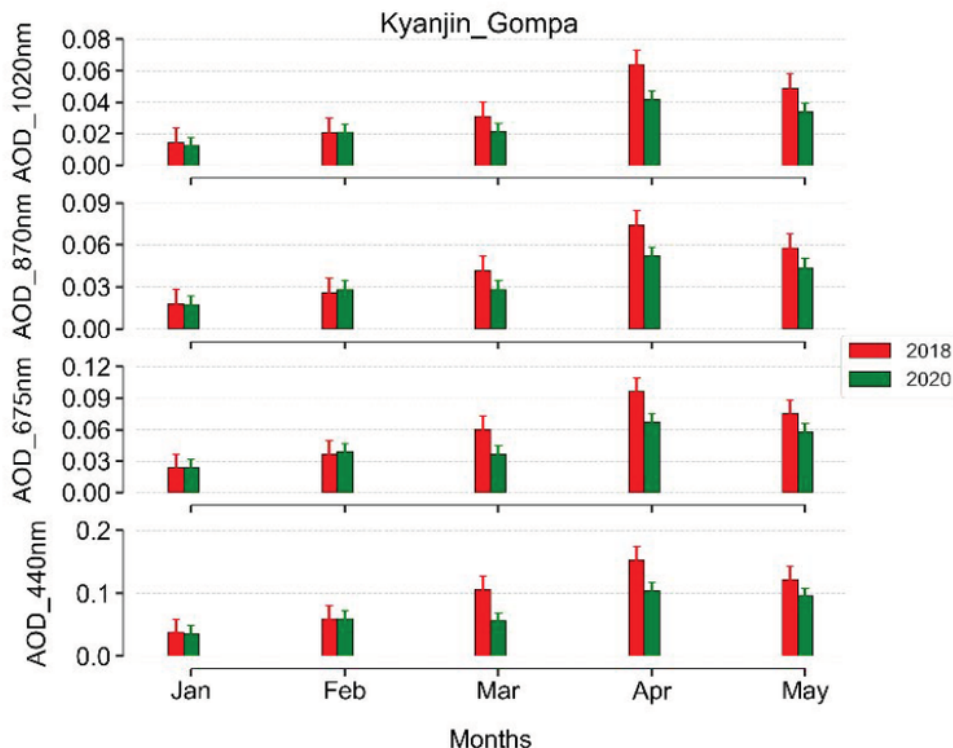


**Figure 4**

AOD monthly average over Kyanjin Gompa during Jan-May, 2018 and 2020 (left) and percentage deviation in AOD in 2020 with respect to 2018 (right). The vertical bar at each data point represents the standard deviation from the mean.

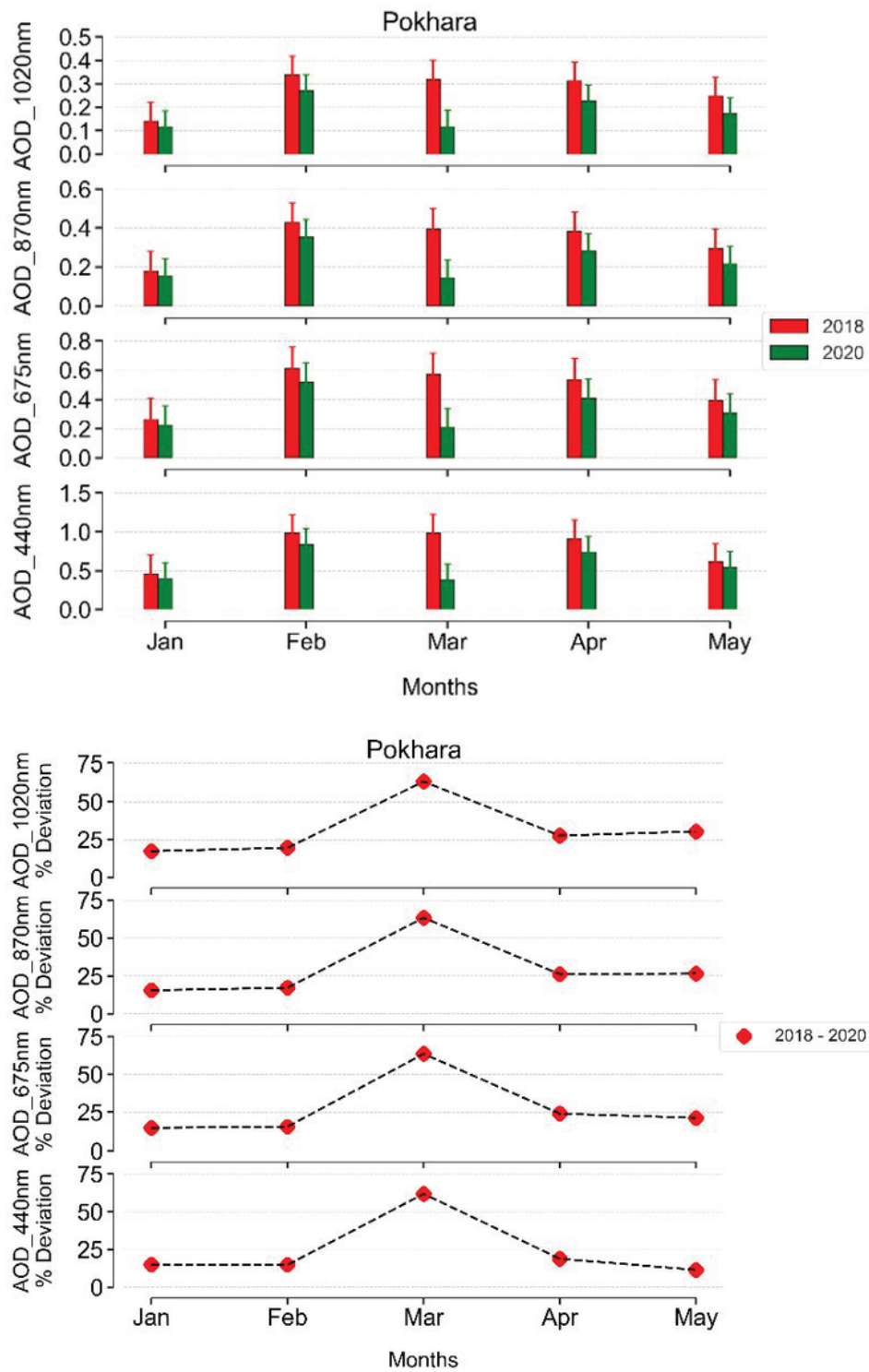


**Figure 5**

AOD monthly average over Pokhara during Jan-May, 2018 and 2020 (left) and percentage deviation in AOD in the year 2020 with respect to 2018 (right).

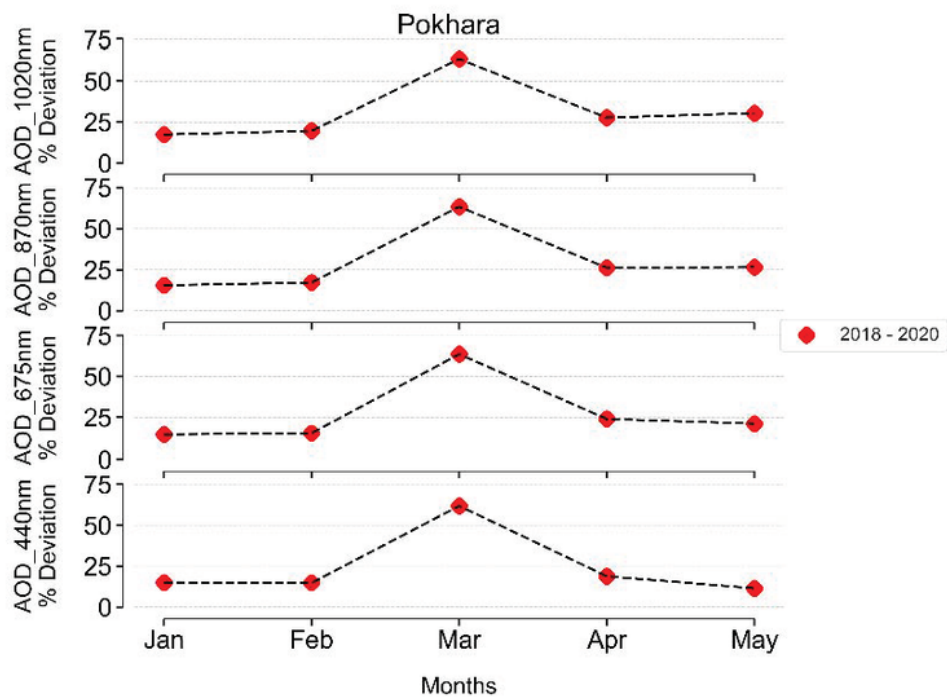
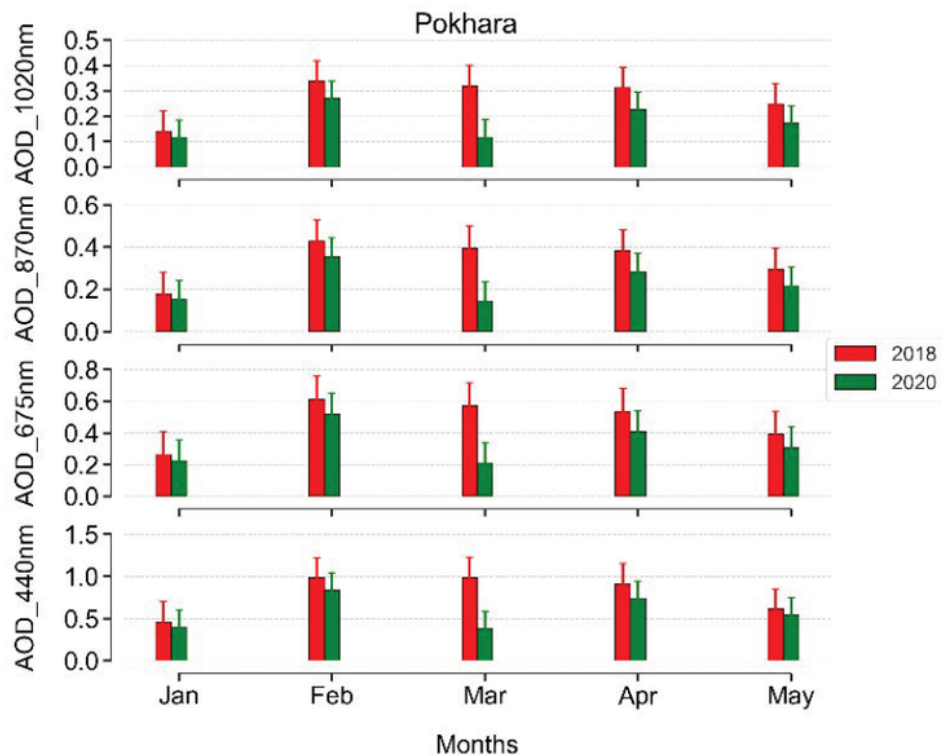


**Figure 6**

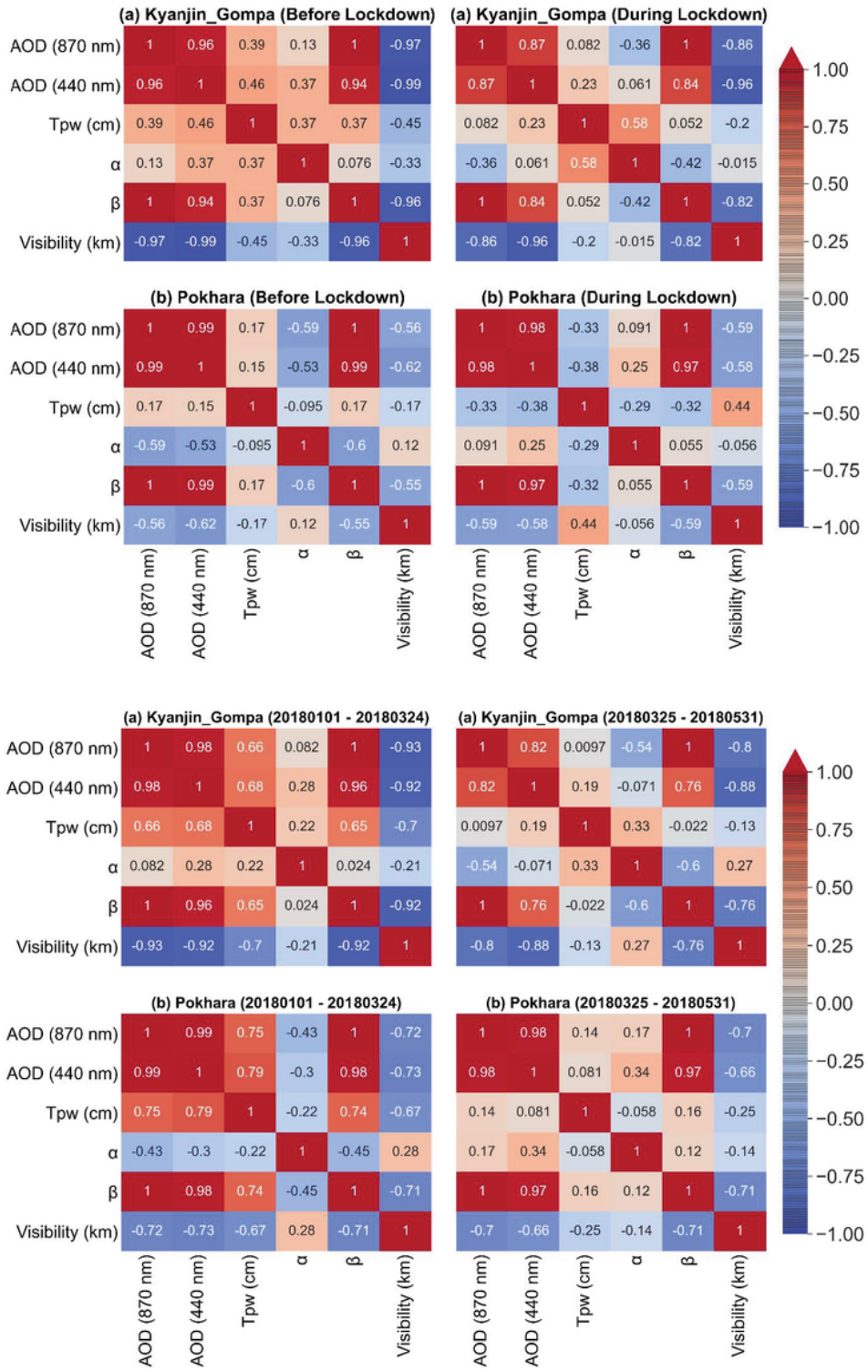


**Figure 6**

Figure shows the correlation coefficients among AOD at wavelengths 870 nm, 440 nm, Total Precipitable Water (Tpw), 440-870 Angstrom Exponent ( $\alpha$ ), Turbidity Coefficient ( $\beta$ ) during Jan-May 2020 (before and after lockdown) over Pokhara and Kyanjin\_Gompa (upper), and the period of Jan-May 2018 over Pokhara and Kyanjin\_Gompa (lower).

Loading [MathJax]/jax/output/CommonHTML/jax.js

## Supplementary Files

This is a list of supplementary files associated with this preprint. Click to download.

- [formulas.docx](#)